Structural Engineering and Mechanics, Vol. 3, No. 3 (1995) 255-272
DOI: http://dx.doi.org/10.12989/sem.1995.3.3.255

Seismic energy dissipation in torsionally responding building systems

J.C. Correnza† and G.L. Hutchinson‡

Department of Civil and Environmental Engineering, The University of Melbourne, Parkville, Victoria 3052, Australia

A.M. Chandler‡†

Department of Civil and Environmental Engineering, University College London, Gower Street, London WC1E 6BT, U.K.

Abstract. The paper considers aspects of the energy dissipation response of selected realistic forms of torsionally balanced and torsionally unbalanced building systems, responding to an ensemble of strong-motion earthquake records. Focus is placed on the proportion of the input seismic energy which is dissipated hysteretically, and the distribution of this energy amongst the various lateral load-resisting structural elements. Systems considered comprise those in which torsional effects are discounted in the design, and systems designed for torsion by typical code-defined procedures as incorporated in the New Zealand seismic standard. It is concluded that torsional response has a fundamentally significant influence on the energy dissipation demand of the critical edge elements, and that therefore the allocation of appropriate levels of yielding strength to these elements is a paramount design consideration. Finally, it is suggested that energy-based response parameters be developed in order to assist evaluations of the effectiveness of code torsional provisions in controlling damage to key structural elements in severe earthquakes.

Key words: energy dissipation; hysteretic behaviour; seismic response; torsional design.

1. Introduction and background

In earthquake-resistant design, economic constraints require that the lateral load-resisting elements of structures be designed to respond inelastically beyond yield. Such structures, if efficiently and effectively designed, will take advantage of the strength reserves present in structural materials in their post-yield range. Static response parameters quantifying the degree of inelastic response, such as the maximum displacement ductility demand (Tso and Zhu 1992, Goel and Chopra 1994), disregard the cyclic response characteristics of the structure when subjected to severe seismic ground motion. In this respect, an important aspect of the efficient design of inelastic structures is their ability to dissipate large quantities of seismic energy, whilst incurring minimal damage. Such energy quantities may be employed as structural response parameters, to comprehend more

† Graduate Student
‡ Professor and Head
‡† Reader in Earthquake Engineering

fully the influence of earthquake characteristics and key structural parameters on the inelastic dynamic behaviour and response of buildings excited by seismic events (Zahrah and Hall 1984, Tembulkar and Nau 1987, Uang and Bertero 1990).

At the cessation of the ground motion and the associated building movements, all the imparted seismic energy must have been totally dissipated by the structure. At any instant during the dynamic response, a proportion of the energy will have been dissipated through structural damping and by the hysteretic behaviour of the load-resisting structural and non-structural components of the building. The dissipation of energy by hysteresis can only occur in the inelastic response range of the structure. The remaining part of the input energy accumulated by that moment in time is instantaneously stored in two forms. These comprise the kinetic energy concentrated in the mass of the idealised floor system(s), and the elastic strain energy in the lateral load supporting walls and columns, as well as in other elements which may be nominally non-structural.

In previous studies of earthquake energy absorption in idealised and simplified structures (referred to above), focus has been placed on the translational (lateral) response of single-degree-of-freedom (SDOF) systems. Such systems possess symmetry in their distributions of mass, lateral stiffness and lateral yield strength, as well as having a symmetric geometric configuration. These studies are necessarily limited because few, if any, realistic buildings are symmetric in all these respects. Asymmetry results in the presence of a structural eccentricity between the centres of mass and lateral stiffness (detailed definitions of structural eccentricities relevant to dynamic response studies are presented in Chandler, *et al.* 1994). Hence the response of all buildings to earthquake-induced loadings (and other forms of dynamic loading) has a lateral and a torsional component; the latter often heavily influences the response of the key load-resisting elements situated at the building perimeter (Chandler, *et al.* 1994, Chandler and Hutchinson 1987). In the design process, therefore, to account for these torsional effects, building codes specify a torsional moment applied to the floor, which is applied when determining the distribution of lateral design strength amongst the load-resisting elements.

This paper considers the inelastic response of selected, typical and realistic torsionally unbalanced building systems. Four key aspects of their behaviour are examined:

(1) The proportion of the input energy which is dissipated hysteretically is established.
(2) The distribution of this energy amongst the various lateral restraining elements is evaluated, for systems designed for torsion according to the New Zealand earthquake standard (Standards Association of New Zealand 1992, designated NZS-92), and for systems in which torsional effects have not been allowed for. In the latter systems, the element strengths are directly proportional to their lateral stiffnesses (termed 'stiffness and strength proportional', or SSP systems).
(3) This hysteretic energy distribution between the various elements is evaluated for systems with a range of natural periods, and comparisons are made between torsionally balanced and unbalanced systems subjected to a series of well-known strong motion earthquake input motions.
(4) Finally, the influence of the magnitude of the structural eccentricity on the hysteretic energy dissipated for the torsionally balanced and unbalanced systems is studied, for the same ensemble of earthquake ground motions.

2. Model definition and ground motion input

A single storey structural model is employed in this paper, as shown in Fig. 1(a), such that

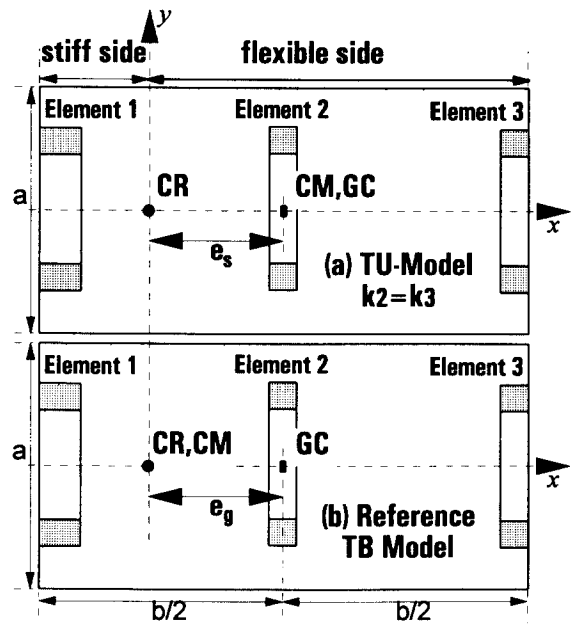

Fig. 1 Plan configurations for (a) torsionally unbalanced (TU) system, and (b) torsionally balanced (TB) reference system.

the lateral y-direction earthquake resistance is provided by three beam-column elements, which in turn support a rigid floor diaphragm of dimensions b and a. It is herein assumed that firstly, the lateral stiffnesses of elements 2 and 3 are equal, and hence the structural system has a moderate level of torsional resistance, and secondly that the plan aspect ratio (defined as $\lambda=b/a$) is equal to 2.0, these properties being representative of prototypical asymmetric buildings (Correnza, *et al.* 1994a). The centre of resistance (stiffness) CR, centre of mass CM and geometric centroid GC are noted along with the structural or static eccentricity e_s.

The stiff and flexible sides of the building are defined. The structural system considered has a uniform (balanced) distribution of mass, and hence CM is coincident with GC. However, the element stiffness distribution is non-uniform and hence the structure is termed torsionally unbalanced (TU), whereby CR is offset from CM and GC by the static eccentricity e_s, which herein is normalised to the plan dimension b, in the form $\grave{e}_s=e_s/b$. For the results presented in this study, TU systems have been considered with large normalised static eccentricity (hence giving significant dynamic torsional response components), corresponding to $\grave{e}_s=0.3$. For reference purposes, corresponding torsionally balanced (TB) systems responding only in translation under laterally-induced earthquake loading are defined, as in Fig. 1(b). This latter system is achieved by modifications such that CM coincides with CR, without altering the values of any other parameters. In the TB system, the position of CR (and CM) with respect to GC is defined by the geometric or CR eccentricity e_g, whose normalised value is taken herein as $\grave{e}_g=e_g/b=0.3$. A more detailed discussion of all aspects of these models, including the definition of relevant torsional stiffness parameters, has been presented in detail in Chandler, *et al.* (1994) and Correnza (1994).

The structural system has been subjected to an ensemble of six strong-motion western U.S. earthquake records (Correnza, *et al.* 1994a), whose 5% damped elastic response spectra correspond closely to the well-known Newmark-Hall smoothed linear elastic design response spectrum, or

SLEDRS (Newmark and Hall 1982). The strong-motion duration of each record is greater than 10 secs, ensuring that several cycles of inelastic response occur in each system. Given that the systems analysed have periods T_y at the extreme ends of the velocity-controlled region of the response spectrum (i.e., 0.5 secs and 2.5 secs), the ground motions have all been normalised to a peak ground velocity V, equal to 0.35 m/s. The 6 earthquake input records have been divided into 3 pairs, according to the value of the ratio A/V (A=peak ground acceleration, in units of g). This ratio influences, amongst other factors, the spectral energy content of earthquake ground motions.

The total lateral design strength F_y is determined for the purposes of inelastic design by direct reduction from the Newmark-Hall SLEDRS, using a force modification factor F_R of 5. This value is compatible with systems designed with high levels of ductility capacity, such as special seismic moment-resisting frames. The force-deformation characteristic of the lateral load-resisting frames is assumed to be bi-linear, with 2% strain hardening in the post-yield range. The justification of this material behaviour model for studies of the present type has been presented by Correnza, *et al.* (1992).

3. Definition of structural energy quantities

To derive the energy equations, and hence the fundamental energy response parameters, analogy is made with a viscously damped bi-linear SDOF system. For this system, the equation of dynamic motion may be written as:

$$m\ddot{u}+c\dot{u}+R_f=-m\ddot{u}_g \tag{1}$$

where m=mass of the structure; c=viscous damping coefficient; R_f=internal restoring force; u=relative displacement of the mass, with respect to the ground, and u_g=the earthquake ground displacement (Note: the absolute or total displacement of the mass is defined as $u_t=u+u_g$). Appropriate differentiation of the above displacements with respect to time results in the corresponding velocity and acceleration quantities, as in Eq. (1).

The earthquake energy imparted to the structure is completely dissipated and absorbed through the various mechanisms referred to in Section 1 above. Integrating the equation of motion (1) with respect to the relative displacement u, gives:

$$\int m\ddot{u}du+\int cudu+\int R_f du=-\int m\ddot{u}_g du \tag{2}$$

The first integral on the left-hand side of Eq. (2) defines the instantaneous kinetic energy E_k, and is equal (Uang and Bertero 1990) to $1/2m\dot{u}^2$, where $\dot{u}$ is the instantaneous velocity of CM, relative to the ground. The second term on the left-hand side represents the damping energy, which is always positive, and is written (Zahrah and Hall 1984) as:

$$E_d=\frac{4\pi\xi m}{T_y}\int \dot{u}^2dt \tag{3}$$

where ξ is the viscous damping ratio (herein taken as 0.05), T_y is the elastic lateral period of the system, and E_d is determined (as with E_k) for the whole structure, with respect to the instantaneous velocity of CM. From the form of Eq. (3), it is observed that the dissipated damping energy is a time-accumulated quantity, which increases as the response history progresses.

Analogous to the kinetic energy, the instantaneous recoverable elastic strain energy, E_s, which is determined with respect to the displacement of CM, is equal (Uang and Bertero 1990) to $R_f^2/2k$, where k is the instantaneous lateral stiffness of the system. This result is obtained from the third integral on the left-hand side of Eq. (2). This integral also gives the dissipated hysteretic energy E_h, which is evaluated as the sum of the areas circumscribed by the R_f versus u graphs, for the various elements. Therefore, the energy dissipated by each structural component (frame elements 1-3), when loaded beyond their yield strength, proportionally contributes to the total E_h dissipated by the entire system. As with the damping energy quantity, E_h is an accumulated quantity, evaluated for each element as the sum of the energy dissipated in each loading cycle.

The proportions of each of the above energy types at any particular instant during earthquake-induced loading, vary for different earthquakes and structural configurations. However, conservation of energy prevails in all cases, and hence the sum of the energy quantities above must equal the total energy input E_i which is defined by the integral on the right-hand side of Eq. (2). This may be summarised as follows:

$$E_k + E_d + E_s + E_h = E_i \tag{4}$$

4. Seismic energy input

The energy quantities defined in Section 3 have been determined directly from the integrals given in Eq. (2). These have been appropriately normalised to the structural mass m, and hence have units of energy per unit mass or $(\text{mm/sec})^2$. In order to study the variation of all the energy quantities over the earthquake loading duration, the SSP model has initially been adopted. Later results presented in Sections 6.2, 7 and 8 are concerned with the corresponding model designed for torsional effects according to the provisions of the New Zealand seismic standard, which is representative of the codified approach to torsional design employed in all the major earthquake building codes. These latter results therefore enable comments to be made in relation to code evaluation, as also given in studies employing a ductility-based response parameter (for example, Tso and Zhu 1992). Furthermore, since the trends discussed below in relation to the time-history of energy response have been found in Correnza (1994) to be consistent for each of the earthquake ground motions in the ensemble referred to in Section 2, results have been given for the representative case of the 1940 El Centro, California earthquake (NS component), as in Figs. 2-9. The example systems consist of the TU ($\grave{e}_s = 0.3$) case, along with its corresponding TB reference system (Fig. 1), each of which are taken with fundamental lateral periods of $T_y = 0.5$ sec (short-period) and 2.5 sec (long-period).

The time-history of the total accumulated seismic input energy, E_i (Eq. (4)), is represented in Figs. 2 and 3 by the uppermost curve. For this ground motion record and others with similar spectral characteristics, the majority of the seismic energy is input to the structures (and correspondingly dissipated and absorbed) within the first 30% of the strong-motion loading duration, which for the El Centro NS record is approximately 27 secs. At the end of the strong-motion duration, the energy input to systems exhibiting torsional inelastic response (TU cases) is found to be somewhat less than for the laterally-responding TB cases, although the redistribution of hysteretic energy dissipation amongst the load-resisting elements (as discussed in Section 5.2 below) is also of major design significance.

Finally, for the El Centro NS record (and others with similar characteristics), comparison of Figs. 2 and 3 shows that the total energy input for short-period systems is generally in the order of 2.0-2.5 times larger than for long-period systems.

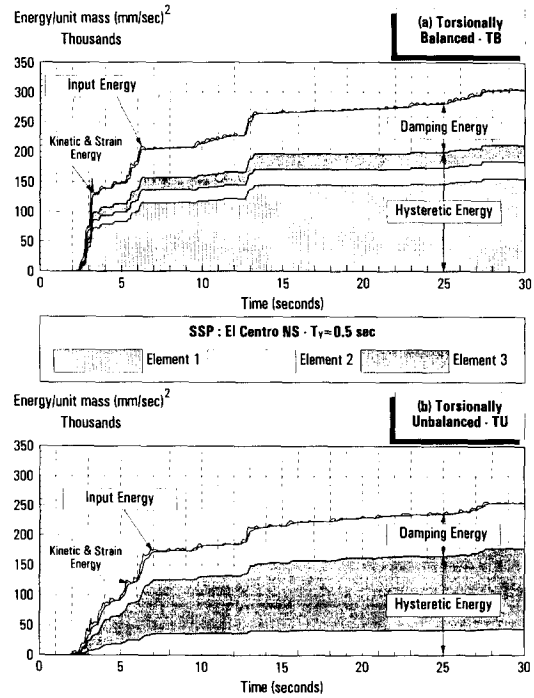

Fig. 2 Time history of energy response for SSP-designed short-period system.

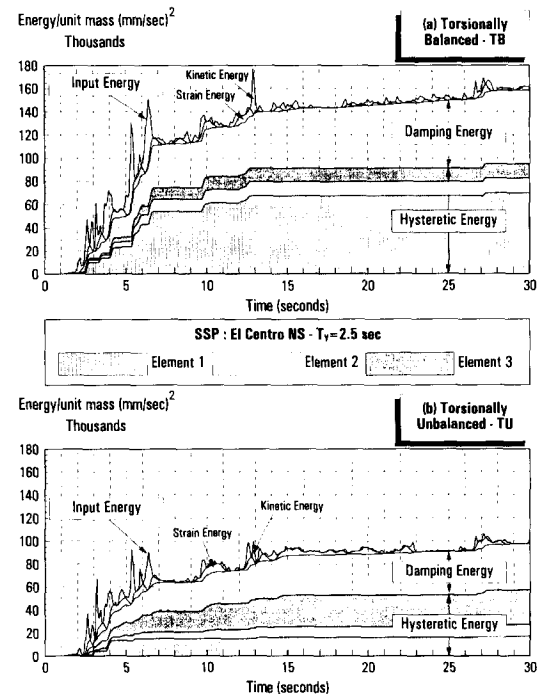

Fig. 3 Time history of energy response for SSP-designed long-period system.

5. Dissipation and absorption of seismic energy

5.1. Strain and kinetic energy components

At the end of the earthquake strong-motion, the structure continues to oscillate in elastic free-vibration. However, the instantaneous strain and kinetic energies associated with these movements are found to be negligible, as indicated on the upper right-hand side of Figs. 2 and 3. Therefore, this implies that all of the imparted seismic energy has been dissipated by a combination of damping action and hysteretic cyclic inelastic response. For short-period systems (Fig. 2), the velocity $\dot{u}$ and displacement u of CM relative to the ground are very small, and correspondingly the instantaneous kinetic and strain energies absorbed by the system are small. This is indicated by the difference between the uppermost curve (input energy) and the curve immediately below. The latter curve, by energy conservation, indicates the total dissipated energy ($E_d + E_h$: Section 5.2). Contrastingly, longer-period systems (Fig. 3) exhibit much higher kinetic and strain energies, as a result of the larger relative movement of CM. Furthermore, the phasing between the kinetic and strain energy response curves is evident in Fig. 3, such that as one quantity reaches its maximum, the other is reduced to zero.

5.2. Damping and hysteretic energy components

As expected in view of the larger relative velocity of CM in the longer-period system (Fig. 3), a greater proportion of the seismic input energy is dissipated by damping action, compared with short-period systems (Fig. 2). Furthermore, the damping energy accumulates at an approximately constant rate over the strong-motion duration in all cases.

The total hysteretic energy dissipated by the structure is composed of contributions from each of the 3 lateral load-resisting elements, when loaded beyond yield. For each yield excursion, hysteretic energy is accumulated and this results in a stepped pattern of increase for this energy quantity, as evident from Figs. 2 and 3. The pattern of the seismic energy input to the system is clearly strongly dependent on the pattern of hysteretic energy accumulation, as seen most clearly for the short-period case (Fig. 2). From an engineering design viewpoint, it is important to quantify the damaging potential of the earthquake with respect to the individual elements. This may be assessed by studying the relative contributions to the total hysteretic energy (E_h) made by each element. This is also related to the yielding sequences and variation of internal element restoring forces, as discussed in detail below.

6. Load duration pattern of hysteretic energy dissipation

For the energy response time-histories illustrated in Figs. 2 and 3, the corresponding variations of element yielding sequences and internal restoring forces have been plotted in Figs. 4-6. For these latter figures, results have been given only for the critical edge elements 1 (stiff-edge) and 3 (flexible-edge). The centrally-located element 2, also on the flexible side of the structure (Fig. 1), gives similar patterns of response to the flexible-edge element 3 (Correnza 1994), but the magnitudes are considerably smaller and hence are not critical for design of flexible-side elements.

For a given system, the initial yield forces of the respective edge elements are stated in Figs. 4-6. For the SSP case, these are proportional to the element stiffnesses, and no account is taken

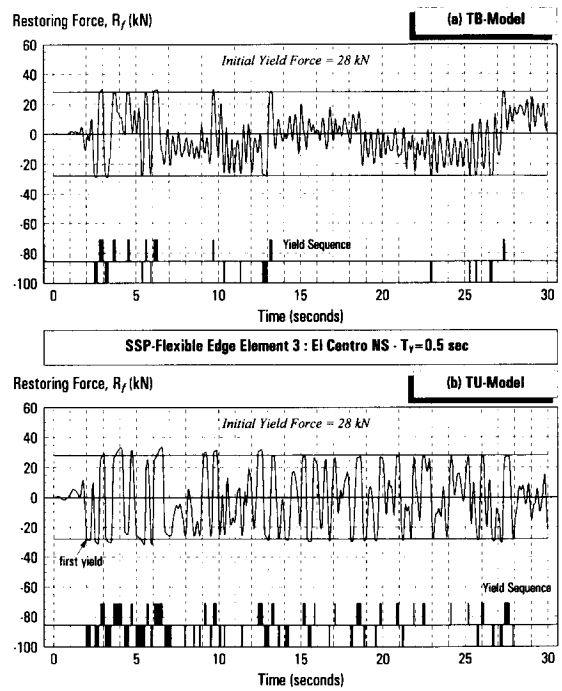

Fig. 4 Time history of element restoring force and yielding sequence for flexible-edge element of SSP-designed short-period system.

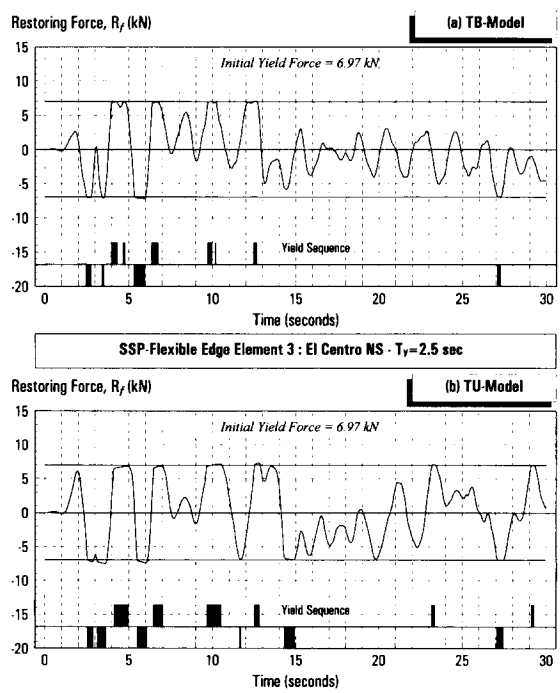

Fig. 5 Time history of element restoring force and yielding sequence for flexible-edge element of SSP-designed long-period system.

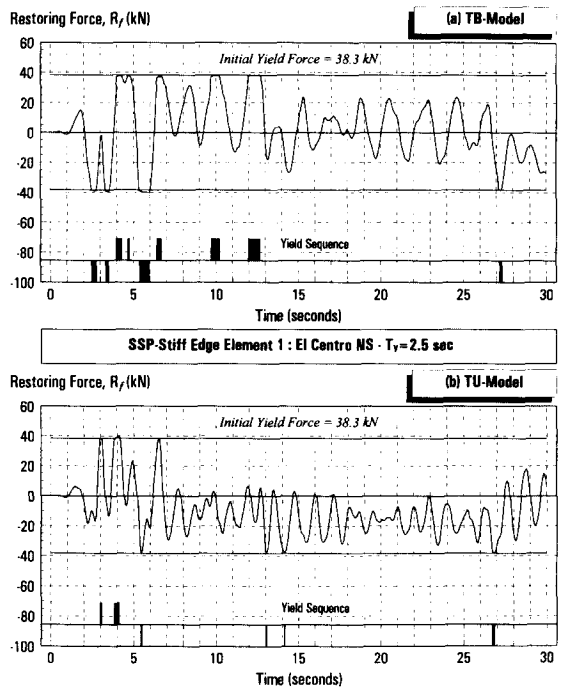

Fig. 6 Time history of element restoring force and yielding sequence for stiff-edge element of SSP-designed long-period system.

of codified torsional design provisions. As a result, the initial yield capacity of the edge elements is the same in both the TB and TU systems. For the short-period TU system in Fig. 4(b), for example, element 3 undergoes its first yield as indicated in the diagram, when the internal element restoring force first reaches the initial yield strength of 28 kN. Subsequently, because of the strain hardening effect incorporated in the bi-linear model, the yield capacity is dependent on the cyclic response behaviour of the element, and hence further yielding occurs at values different from the initial yield force. The differences for the adopted model are small, and are indicated by the element restoring force responses plotted in Figs. 4-6.

6.1. SSP model

For the laterally-responding TB cases (Figs. 2(a) and 3(a)), each element undergoes an identical pattern of yield sequences. Furthermore, the amount of hysteretic energy dissipated by elements 2 and 3 is identical, since their stiffness and strength properties are equal. Despite the identical number of yield excursions in element 1, compared with the flexible-side elements, its higher stiffness and strength results in a proportionally higher contribution to the total hysteretic energy dissipated.

To assess the influence of torsion on the pattern of hysteretic energy dissipation amongst the elements, the short-period system is first examined, as presented in Figs. 2 and 4. In Fig. 4, focus is placed on the response of element 3, which demonstrates significant increases in both the number of yield excursions and their duration in the TU case (b), compared with the TB reference model (a). This increased response, arising from torsional effects, makes the

flexible-edge element more vulnerable to earthquake damage. This is clearly shown in Fig. 2, whereby for this element E_h in the TU system is up to five times greater than for the TB case. For this same case, the so-called 'beneficial effects' of torsion are apparent for the stiff-edge element 1, in that no yielding occurs in this element in the short-period TU system (Fig. 2(b)). The comments made for the short-period system are also generally applicable for long-period cases, as shown in Figs. 3, 5 and 6. Worthy of note is that the stiff-edge element undergoes some yield excursions in the long-period TU system (Fig. 6(b)), although their number and duration remains considerably smaller than in the corresponding TB system without torsion (Fig. 6(a)). The corresponding reduction of E_h dissipated by this element is by a factor of about 4 (Fig. 3). For element 3, an increase in the number of yield excursions due to torsion is apparent (Fig. 5), and their duration is significantly longer. This gives an increase of about 3 times in E_h dissipated by element 3 (Fig. 3).

6.2. NZS-designed model

Analysis has been made of energy dissipation patterns in a long-period (T_v=2.5 sec) TU system having identical properties to the SSP case discussed above, but designed with a strength distribution obtained according to the seismic torsional regulations of the Standards Association of New Zealand (1992). These provisions (Chandler, *et al.* 1994) affect the element strength distribution, to give added protection to the flexible-edge element whilst taking advantage of the expected beneficial influence of torsional response on the stiff-edge element by permitting a reduction of its design yield strength. The codified increase of element 3 strength is by a ratio of 24.6/6.97=3.5 (compare Figs. 8(b) and 5(b)), and the corresponding reduction of element 1 strength is by a ratio 26.2/38.3=0.7 (Figs. 9(b) and 6(b)).

In the TB case, the New Zealand code design provisions (in common with other leading seismic codes) require that element strengths be increased throughout the structure (compared with the SSP case), to account for so-called accidental torsional effects (Correnza, *et al.* 1992). Comparing the initial yield forces given in part (a) of Figs. 8 and 9 with the corresponding cases in Figs. 5 and 6, shows that this increase for accidental torsional effects is by the ratio 11.4/6.97=1.64 for the flexible-edge element 3, and 44.4/38.3=1.16 for the stiff-edge element 1. The larger increase for element 3 accounts for its greater vulnerability to torsional effects, resulting from its location furthest distant from the centre of resistance (stiffness) CR, as in Fig. 1. Consequently, comparing the New Zealand code-designed TB case with the SSP-designed TB case shows that the yield sequences are significantly different, with the number of yield excursions being decreased for both elements 1 and 3. For element 3, this number reduces from 10 to 3. Furthermore, for similar reasons the total hysteretic energy E_h dissipated by the code-designed TB system (Fig. 7(a)) is about 20% less than for the SSP-designed TB system (Fig. 3(a)). However, the distribution of E_h amongst the three elements is not noticeably affected by the inclusion of the accidental eccentricity, with element 1 contributing the majority of the total hysteretic energy dissipated.

The effects of implementing the code torsional provisions are by comparing the performance of the edge elements 1 and 3 in the long-period TU systems of Figs. 7-9 (NZS-92), with the same elements in Figs. 3, 5 and 6 (SSP). For element 3, the factored strength increase of 3.5 (see above) reduces dramatically the number of yield excursions (from 12 to 1), and consequently the proportion of hysteretic energy dissipated by this element is very small in the code-designed system (Fig. 7(b)). Hence with respect to the flexible-edge element, the code objective of reducing torsion-related response (and consequent damage) is clearly met satisfactorily, as also concluded

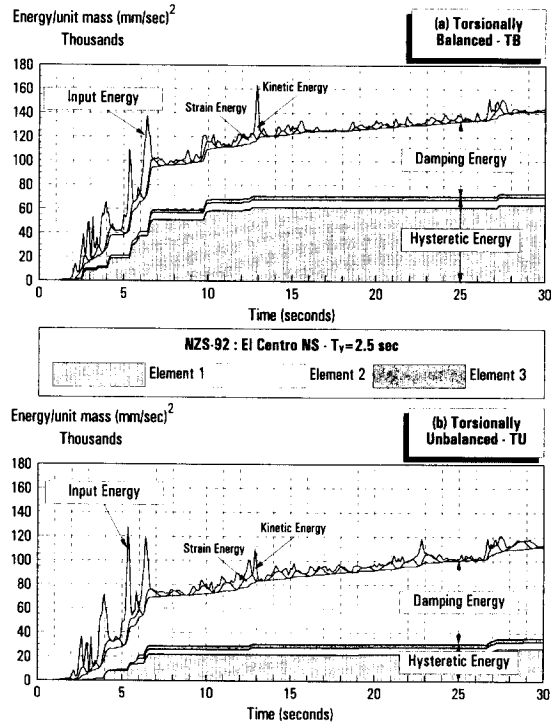

Fig. 7 Time history of energy response for NZS-designed long-period system.

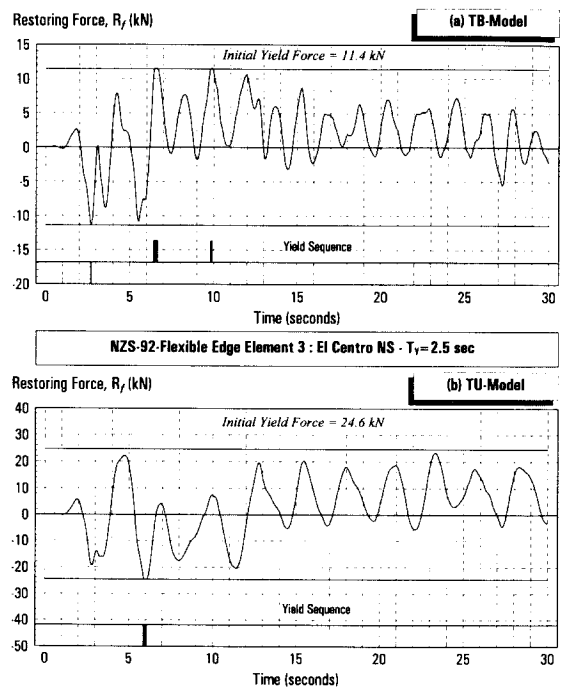

Fig. 8 Time history of element restoring force and yielding sequence for flexible-edge element of NZS-designed long-period system.

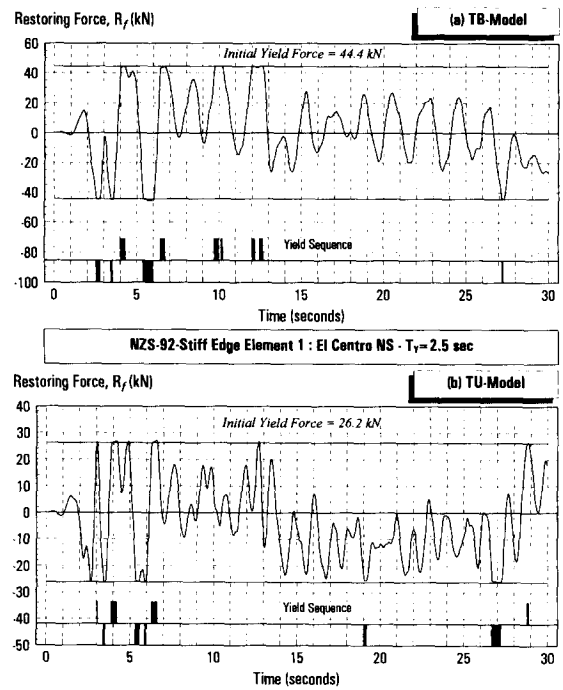

Fig. 9 Time history of element restoring force and yielding sequence for stiff-edge element of NZS-designed long-period system.

by Tso and Zhu (1992) and Chandler, *et al.* (1994). However, the same cannot be said of the performance of the stiff-edge element 1. For this element, the codified strength reduction of 30% referred to above, leads to increases in both the number of yield excursions (from 6 in the SSP case to 9 in the code-designed system), and also in the proportion of hysteretic energy dissipated by this element. In respect of the latter measure of response, element 1 dissipates around 75% of E_h in the code-designed system (Fig. 7(b)), and may therefore by vulnerable to increased damage. This deduction is also compatible with the conclusions of the ductility-based research studies referred to above. Finally, it is noted that the overall increase of lateral strength (known as overstrength) in the code-designed system, which arises partly from the allowance for dynamic torsional effects and also from the accidental torsional provisions, leads to a reduction of the hysteretic energy dissipated by around 40% (compare Figs. 3(b) and 7(b)).

7. Hysteretic energy spectra

As previously mentioned, the general characteristics of the distribution of energy, as identified in the time-histories presented earlier, are applicable to a wide range of earthquake ground motions with various properties. However, the pattern of yielding sequence and therefore the energy absorption and dissipation are highly dependent upon the earthquake event and its particular characteristics (Correnza 1994). Therefore the effect of the ensemble of six earthquake events on the hysteretic energy E_h dissipated in the TB and TU model configurations has been studied (Figs. 10 and 11), and the individual contributions of each element to E_h identified for a sample of three records (Fig. 12). In this latter figure, the quantity H_i is referred to as

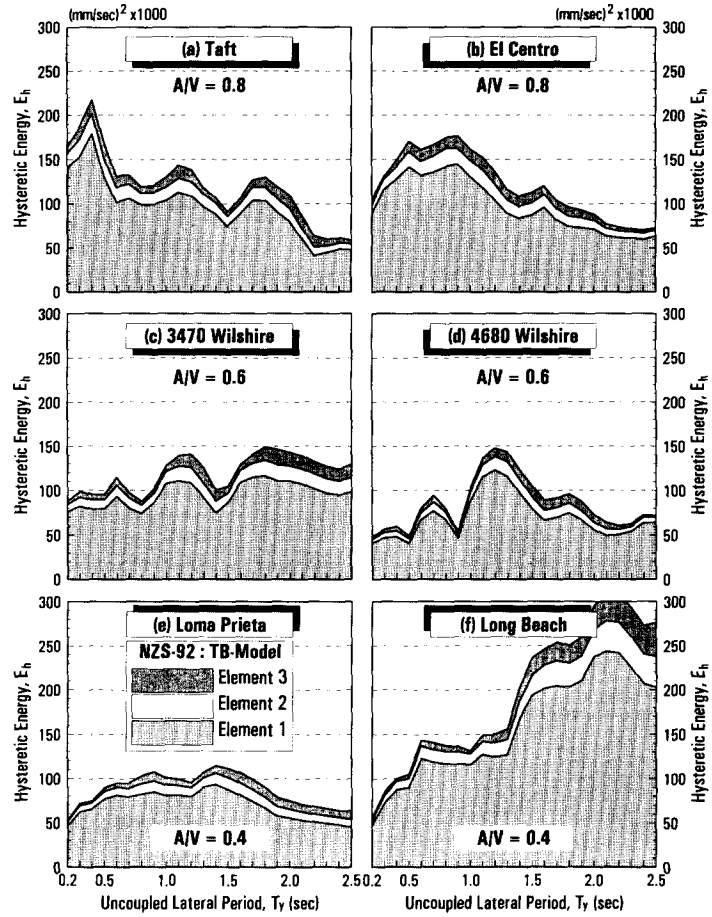

Fig. 10 Hysteretic energy spectra for lateral elements in NZS-designed TB systems subjected to an ensemble of earthquake ground motions.

the proportional hysteretic energy ratio, where i is the element number (1, 2 or 3). This parameter is the ratio of the hysteretic energy dissipated by a particular element, to the total hysteretic energy E_h dissipated by the system.

These studies have been conducted employing the New Zealand (NZS-92) torsional code provision to distribute the lateral element strengths, and the variations in E_h are presented for systems with moderately large stiffness asymmetry ($\grave{e}_s$=0.3) as energy spectra, for systems with a range of fundamental lateral periods (T_y=0.2-2.5 secs). The earthquake records utilised have been divided according to Section 2 into 3 pairs, such that in Figs. 10-12, the records in parts (a) and (b) have moderate values of the ratio A/V, records in parts (c) and (d) have intermediate A/V and records in parts (e) and (f) have low A/V. In general terms, systems with short periods have a tendency to respond more severely to records with higher A/V, whereas systems with long periods tend to have higher response when subjected to records with lower values of A/V.

For the TB system (Fig. 10), it is noted that the stiff-edge element 1 dissipates most of E_h, whereas elements on the flexible side (2 and 3) dissipate relatively small but approximately equal amounts of energy over the period range considered. This is further clarified by results given on the left-hand side of Fig. 12, which correspond to three selected records shown in

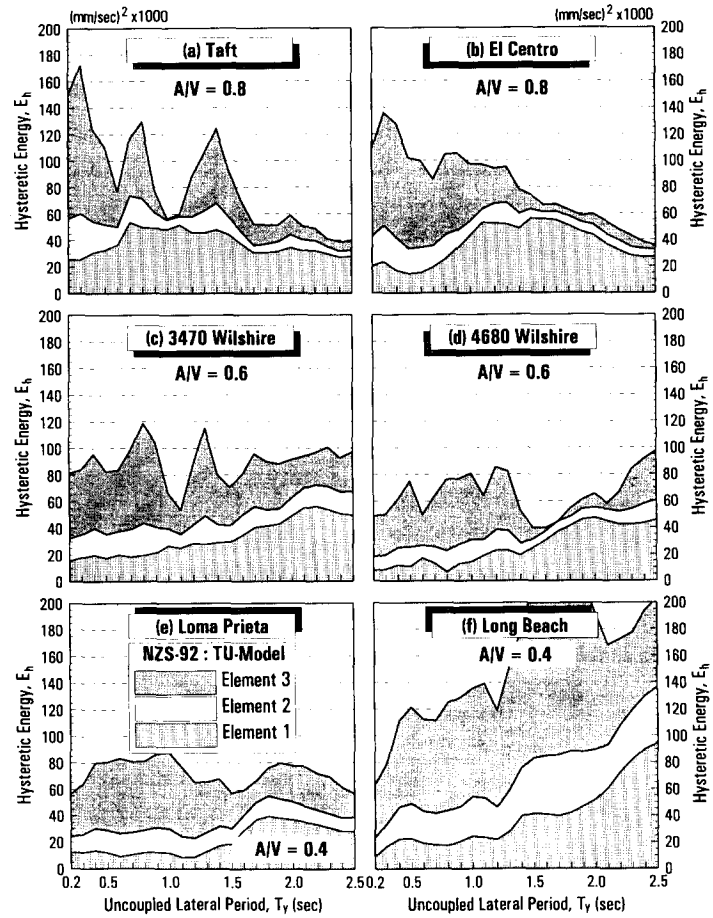

Fig. 11 Hysteretic energy spectra for lateral elements in NZS-designed TU systems subjected to an ensemble of earthquake ground motions.

Fig. 10 (one record for each A/V category). Fig. 12 shows that for the TB case, 75-90% of E_h is associated with the yielding of the stiff-edge element 1. The elements located on the flexible side of the structure each contribute about 5-10% of E_h.

The general trends of dissipated hysteretic energy with period are similar for TU systems (Fig. 11), compared with the reference TB cases (Fig. 10), although the total E_h dissipated is considerably smaller (by 20-40%) in the code-designed TU systems, for the reasons discussed in Section 6 above. With regard to the proportion H_i contributed by each of the elements in TU systems towards the total hysteretic energy dissipated by the structure, the results presented on the right-hand side of Fig. 12 show that there is considerable variation depending on the system period and the earthquake category (A/V ratio). For short-period systems with $T_y<0.8$ sec, subjected to the El Centro record with moderate A/V (=0.8), element 3 contributes roughly 60% of the hysteretic energy dissipated. The same ratio applies within the wider period range $T_y<1.2$ sec, for systems subjected to the 4680 Wilshire record ($A/V=0.6$), and the corresponding period range is further extended to $T_y<1.8$ sec for the Long Beach record ($A/V=0.4$). In the same period ranges, element 1 yields only slightly and contributes around 20% of the hysteretic energy dissipated by the system. For systems with periods longer than those given above, element

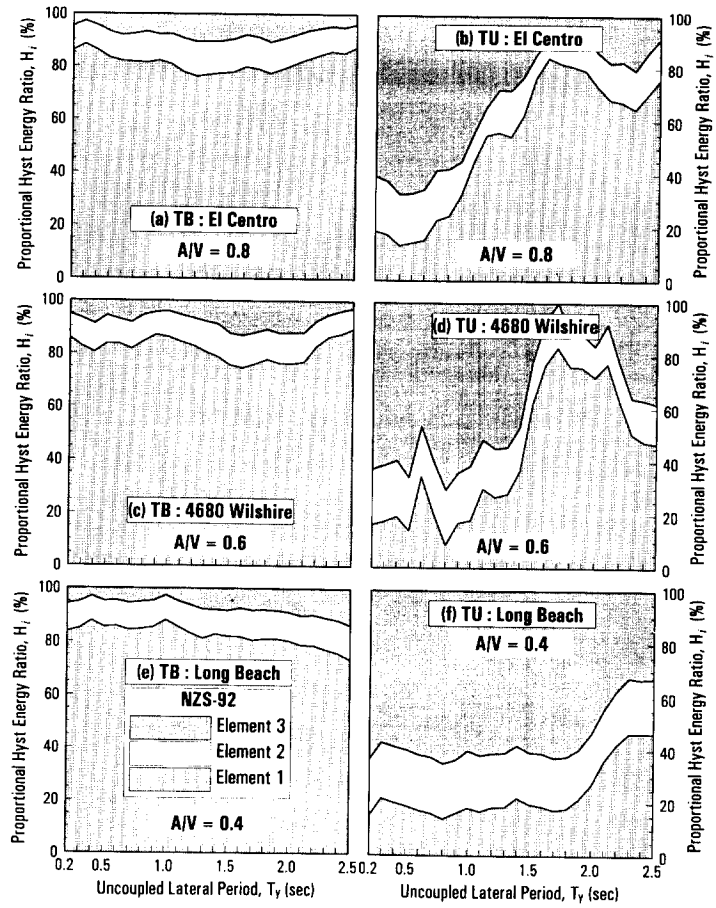

Fig. 12 Proportional hysteretic energy spectra for lateral elements in NZS-designed TB and TU systems subjected to selected earthquake ground motions.

1 increases its extent of yielding (H_1), with a compensating reduction in H_3. However, H_2 remains approximately constant throughout the full period range. These trends highlight the period-dependency of inelastic torsional effects, as discussed in greater detail in Chandler, *et al.* (1994).

8. Influence of structural eccentricity on hysteretic energy

An investigation has been made of the effect of varying the level of stiffness eccentricity, on the total hysteretic energy dissipated and its composition with respect to element energy dissipation, for TB and TU systems designed according to the New Zealand (NZS-92) static code torsional provisions. These systems have been analysed in response to the three selected earthquake events with a range of A/V ratios, as referred to in Section 7. The results are presented in Fig. 13 for short-period systems (T_Y=0.5 sec), and results for systems with longer periods have been presented in Correnza (1994).

For the TB system (left-hand side of Fig. 13), the normalised CR eccentricity $\grave{e}_g$ defines the position of CR with respect to GC, as in Fig. 1(b). For the symmetric case with $\grave{e}_g$=0, the

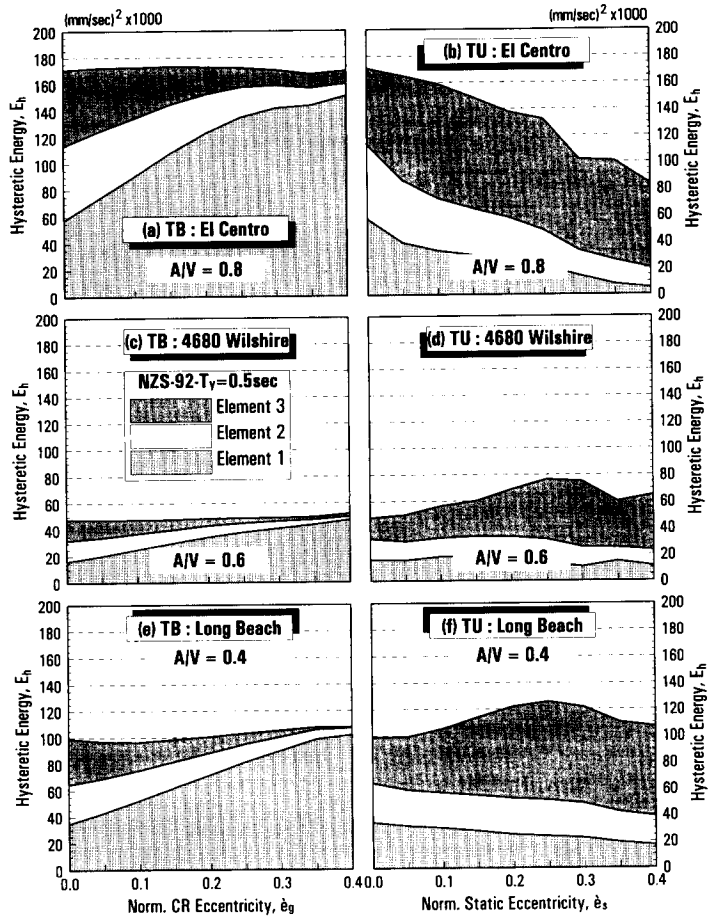

Fig. 13 Effect of eccentricity on the hysteretic energy dissipated in lateral elements in NZS-designed short-period TU and TB systems subjected to selected earthquake ground motions.

properties of all elements are identical, and hence each element contributes equally towards E_h. With increasing $\grave{e}_g$, the strength amplifying effects of the accidental torsional provisions, described in Section 6.2 above, cause the hysteretic energy dissipated by elements 2 and 3 to reduce, and their contribution becomes negligible for highly eccentric systems with $\grave{e}_g=0.4$. Conversely, although the accidental torsional provisions amplify the strength of element 1, this effect is greatest when the system is symmetric, i.e., for $\grave{e}_g=0$, for which the lever arm between the stiff-edge element and CR is greatest. Therefore, the contribution of hysteretic energy dissipated by element 1 increases rapidly as $\grave{e}_g$ becomes larger.

For the TU case (right-hand side of Fig. 13), increasing the normalised static eccentricity $\grave{e}_s$ causes a reduction in E_h for systems subjected to the *E*1 Centro record ($A/V=0.8$). Contrastingly, the hysteretic energy dissipated E_h shows slight increases with larger $\grave{e}_s$ for systems subjected to records with $A/V=0.6$ and 0.4. As $\grave{e}_s$ increases, the contribution of element 3 to E_h increases and that of element 1 decreases, but the contribution of element 2 remains approximately constant. The presentation of results in all earlier figures for the case $\grave{e}_s=0.3$ appears to be justified, on the basis that neither the hysteretic energy dissipated, nor its distribution amongst the elements, are as sensitive to variations in eccentricity, compared with variations in lateral period or the

category of earthquake input record.

9. Application to damage estimation

Previous studies (Park and Ang 1985, McCabe and Hall 1989) have incorporated energy-based parameters and the total number of yield excursions to derive damage models or indices for application in design procedures or in analytical and experimental research. The results presented in the current paper indicate the potential for extending this approach to torsionally responding inelastic systems, in order to define energy-related damage indices for the critical edge elements in such systems. These indices have the potential to provide information for evaluating the efficiency and effectiveness of code torsional provisions, particularly in preventing excessive damage for ultimate limit state design of torsionally-responding systems subjected to severe earthquakes. Comparisons with existing code evaluation studies (Tso and Zhu 1992, Chandler, *et al.* 1994, Goel and Chopra 1994) based on inelastic ductility and deformation demands would then be feasible, to obtain a more complete code assessment procedure. Studies are currently being carried out towards this objective and some preliminary results have been included in Correnza (1994).

10. Conclusions

The studies presented in this paper have employed energy response parameters to assess the effect of various earthquake events, structural configurations and fundamental system parameters on the inelastic response of torsionally balanced and unbalanced structural models. The latter have included both the stiffness and strength proportional case, and a typical code-designed torsionally-responding system. The energy imparted to structures by earthquake-induced loading has been investigated, by considering its breakdown into instantaneous (or absorptive) components and dissipative components. Of the latter type, the hysteretic energy is indicative of the damaging potential of a given ground motion, and for torsionally responding systems the distribution of hysteretic energy amongst the resisting elements permits assessments firstly of response characteristics in eccentric systems, and secondly an evaluation of the effectiveness of code torsional provisions.

The introduction of torsional response has been observed to have a very significant influence on the energy response behaviour of inelastic systems. Of particular note is the re-distribution of hysteretic energy dissipation, such that for torsionally unbalanced systems, elements on the flexible side of the building (and especially the flexible-edge element) dissipate almost all of the hysteretic energy of the entire system. This is in contrast to the laterally-responding torsionally balanced reference system, with stiffness distribution identical to the torsionally unbalanced system, which relies on a very high contribution from the stiff-edge element towards the dissipation of imparted seismic energy. These effects have been observed both for systems designed for torsional effects, and to a greater extent for systems in which element design strengths take no account of changes arising due to torsional response.

The total hysteretic energy dissipated by both laterally-responding and torsionally-responding systems, and its distribution amongst the lateral load-resisting elements, have been studied in the form of energy response spectra. The total hysteretic dissipated energy is influenced to a similar degree in both forms of system, by variation of the ground motion A/V ratio. Whilst the relative contributions of elements to the hysteretic energy dissipated by the system remain almost constant with lateral period for torsionally balanced systems, in code-designed torsionally

unbalanced cases the energy is largely dissipated by the flexible-edge element in short-period systems whilst the stiff-edge element contributes significantly only in longer-period systems.

The inclusion of codified accidental eccentricity provisions in determining element design strengths for the torsionally balanced case causes the contribution to energy dissipation made by the flexible-side elements to decrease as the eccentricity of the stiffness centre increases, and this effect is substantially compensated by an increase in the contribution from the stiff-side element. For the corresponding torsionally unbalanced code-designed system, the increase of static eccentricity causes the flexible-edge element to increase significantly its contribution to hysteretic energy dissipation, whilst the contribution of the stiff-edge element correspondingly reduces as the beneficial effects of torsional response become apparent. The need to protect the flexible-edge element in torsionally-responding systems by specifying a sufficient increase in its design yield strength is therefore paramount.

Finally, it is suggested that energy-based response parameters be developed in order to assist evaluations of the effectiveness of code torsional provisions in controlling damage to key structural elements in severe earthquakes.

References

Chandler, A.M. and Hutchinson, G.L. (1987), "Evaluation of code torsional provisions by a time history approach", *Earthquake Engineering and Structural Dynamics*, **15**, 491-516.

Chandler, A.M., Correnza, J.C. and Hutchinson, G.L. (1994), "Period-dependent effects in seismic torsional response of code systems", *Journal of Structural Engineering ASCE*, **120**(12), 3418-3434.

Correnza, J.C., Hutchinson, G.L. and Chandler, A.M. (1992), "A review of reference models for assessing inelastic seismic torsional effects in buildings", *Soil Dynamics and Earthquake Engineering*, **11**(8), 465-484.

Correnza, J.C. (1994), "Inelastic dynamic response of asymmetric structures subject to uni- and bi-directional seismic ground motions", *Ph.D thesis*, The University of Melbourne, Australia.

Correnza, J.C., Hutchinson, G.L. and Chandler, A.M. (1994a), "Effect of transverse load-resisting elements on inelastic earthquake response of eccentric-plan buildings", *Earthquake Engineering and Structural Dynamics*, **23**(1), 75-89.

Correnza, J.C., Hutchinson, G.L. and Chandler, A.M. (1994b), "Inelastic response of the flexible-edge element in code-designed eccentric structures", *5th U.S. National Conference on Earthquake Engineering*, **1**(AB-3), 169-178, Chicago, July.

Goel, R.K. and Chopra, A.K. (1994), "Dual level approach for seismic design of asymmetric-plan buildings", *Journal of Structural Engineering ASCE*, **120**(1), 161-179.

McCabe, S.L. and Hall, W.J. (1989), "Assessment of seismic structural damage", *Journal of Structural Engineering ASCE*, **115**(9), 2166-2183.

Newmark, N.M. and Hall, W.J. (1982), *Earthquake spectra and design*, Monograph Series, **3**, Earthquake Engineering Research Institute, CA.

Park, Y.J. and Ang, A.H.-S. (1985), "Mechanistic seismic damage model for reinforced concrete", *Journal of Structural Engineering ASCE*, **111**(4), 722-739.

Standards Association of New Zealand (1992), Code of practice for general structural design and design loadings for buildings, NZS:4203, Wellington, New Zealand.

Tembulkar, J.M. and Nau, J.M. (1987), "Inelastic modelling and seismic energy dissipation", *Journal of Structural Engineering ASCE*, **113**(6), 1373-1377.

Tso, W.K. and Zhu, T.J. (1992), "Design of torsionally unbalanced structural systems based on code provisions I: Ductility demand", *Earthquake Engineering and Structural Dynamics*, **21**, 609-627.

Uang, C.M. and Bertero, V.V. (1990), "Evaluation of seismic energy in structures", *Earthquake Engineering and Structural Dynamics*, **19**, 77-90.

Zahrah, T.F. and Hall, W.J. (1984), "Earthquake energy absorption in SDOF structures", *Journal of Structural Engineering ASCE*, **110**(8), 1757-1772.